iJRASET
International Journal For Research in Applied Science and Engineering Technology



INTERNATIONAL JOURNAL FOR RESEARCH

IN APPLIED SCIENCE & ENGINEERING TECHNOLOGY

Volume: 13 **Issue:** IX **Month of publication:** September 2025

DOI: https://doi.org/10.22214/ijraset.2025.74375

www.ijraset.com

Call: 08813907089 | E-mail ID: ijraset@gmail.com

International Journal for Research in Applied Science & Engineering Technology (IJRASET)
ISSN: 2321-9653; IC Value: 45.98; SJ Impact Factor: 7.538
Volume 13 Issue IX Sep 2025- Available at www.ijraset.com

Effect of ZnSe andCdS Shells on the Structural and Photophysical Behavior of CdSe Nanocrystals in a PVA Matrix

Pisal Mahadeo Bhiku[1], Dr. Shailendra Jain[2]
[1]*Research Scholar,* [2]*Professor, Department of Physics, Eklavya University, Damoh, M.P*

Abstract: ***The CdSe nanocrystals implanted in a polyvinyl alcohol (PVA) matrix are examined in this work to determine the influence of ZnSe and CdS shells on their structural and photophysical behavior. By using a controlled experimental methodology, we were able to synthesis four different sets of samples using the same base conditions and systematically varying just the shell composition. There were a total of 125 samples distributed throughout the categories, which comprised bare CdSe cores, CdSe/ZnSe single-shell, CdSe/CdS single-shell, and CdSe/ZnSe/CdS double-shell nanocrystals. The structural investigation, which included TEM and XRD, verified that the particle size and crystallite domains increased gradually during shelling, and that lattice strain decreased, suggesting an improvement in crystal quality. Quantum yield rose dramatically from bare CdSe to double-shelled samples, and optical measurements showed that absorption and emission peaks shifted red as the photoluminescence full width at half maximum (FWHM) shrank. The results of the time-resolved PL analysis demonstrated that the improved surface passivation led to longer lifetimes and the suppression of non-radiative decay channels. Shelling also significantly enhanced PVA's photostability, thermal resistance, film smoothness, and environmental robustness, according to stability evaluations. In addition to improving the structural integrity and environmental stability of CdSe nanocrystals, our results show that ZnSe and CdS shells increase luminescence efficiency, suggesting that these materials might be used in optoelectronic and photonic applications.***

Keywords: CdS shell, photophysical behavior, PVA matrix, structural properties, quantum dots.

I. INTRODUCTION

In the last twenty years, semiconductor nanocrystals, or quantum dots (QDs), have been the center of a lot of research interest because of the optical and electrical characteristics that vary with size. The variable bandgap, strong quantum confinement effect, and high photoluminescence (PL) efficiency of cadmium selenide (CdSe) nanocrystals make them one of the most researched systems among these. They have many different uses, including in bio-imaging and sensing as well as in light-emitting diodes and solar cells. But photo-oxidation, surface flaws, and poor chemical stability are common issues with bare CdSe nanocrystals, resulting in PL quenching and diminished device performance. A hopeful approach to improving the stability and photophysical characteristics of CdSe nanocrystals has been the development of core/shell nanostructures, in which CdSe serves as the core and is passivated by a semiconductor shell, such as zinc selenide (ZnSe) or cadmium sulfide (CdS). This structure has the potential to overcome these constraints. Providing a lattice-matched overlayer that shields the core from non-radiative recombination routes is the principal role of a shell material in CdSe-based nanocrystals in passivating surface states. The appealing band orientations of ZnSe and CdSe make them ideal candidates for CdSe shells. The bandgap of ZnSe is around 2.7 eV, which is greater than that of CdSe at 1.74 eV. This broader bandgap efficiently traps electrons and holes within the CdSe core, making the PL intensity and stability better. Just like CdS, which has a bandgap of around 2.42 eV, it provides an alternative confinement situation that permits charge carrier partial delocalization, which might result in red-shifted emission and enhanced quantum yield. Therefore, the photophysical behavior of CdSe nanocrystals may be tuned by selecting either a ZnSe or CdS shell.

Equally crucial are the structural properties of core/shell nanocrystals. The surface chemistry, crystal structure, and morphology are all affected by shell growth. As an example, the optical transitions, size development, defect generation, and core-shell interface strain are all impacted by the CdSe-shell lattice mismatch. ZnSe is more suited for coherent shell formation and dislocation minimization because to its lesser lattice misfit with CdSe (~6.7%) compared to CdS (~4%). The strain-induced widening of PL spectra is a trade-off for the increased protection against photo-degradation that thicker CdS shells may provide.

©IJRASET: All Rights are Reserved

Hence, the relationship between structural integrity and photophysical performance may be better understood by comparing the ZnSe and CdS shells in CdSe nanocrystals. Nanocrystals of CdSe/ZnSe and CdSe/CdS embedded in a polyvinyl alcohol (PVA) matrix have their applications multiplied. One such flexible host media is polyvinyl alcohol (PVA), a water-soluble, transparent, and chemically durable polymer. Several benefits accrue from embedding nanocrystals in PVA, including enhanced environmental stability, better dispersion, and prevention of agglomeration. In addition, thin films that can be solution-processed are possible thanks to the polymer matrix, making them ideal for use in bio-imaging platforms and optoelectronic devices. The combination of core/shell passivation and polymer encapsulation creates a strong system that may be used to explore basic photophysical characteristics as well as their practical applications. The photophysical properties of core/shell nanocrystals, especially their photoluminescence (PL) properties, provide important details regarding the dynamics of carriers, the paths for exciton recombination, and the defect states. Surface defect passivation and confinement effects usually lead to an increased PL quantum yield when ZnSe and CdS shells are grown.

On the other hand, their effects on the emission wavelength, line broadening, and intensity changes are distinct. In contrast to CdS shells, which often cause a redshift and widening in emission due to carrier delocalization and strain effects, ZnSe shells typically retain a sharp and strong emission peak with decreased trap-assisted recombination. PL studies that account for time also show that exciton durations vary, which sheds light on the processes of recombination. Nanocrystal design optimization for targeted optoelectronic applications requires such comparison analysis. Shell growth changes crystal structure, size distribution, and surface chemistry; structural experiments utilizing X-ray diffraction (XRD), transmission electron microscopy (TEM), and Fourier-transform infrared (FTIR) spectroscopy, among others, show this. Embedded CdSe/ZnSe and CdSe/CdS nanocrystals in PVA display unique bonding interactions, strain relaxation patterns, and crystallinity. The correlation between these structural changes and the photophysical trends highlights how morphology and optical characteristics in these hybrid nanomaterials are interconnected. Looking at CdSe nanocrystals in a PVA matrix with ZnSe and CdS shells offers a holistic view of how material design affects photophysical and structural behavior. In contrast to ZnSe shells, which place an emphasis on coherent lattice matching and crisp emission, CdS shells bring broader emission spectra and larger passivation layers. A viable option for improving performance in photonic and electrical applications is to embed in PVA, which stabilizes these properties. In addition to laying the groundwork for the fabrication of cutting-edge nanocrystal-based technologies, these systematic research enhance our basic knowledge of core/shell interactions.

II. LITERATURE REVIEW

Boro, Pallabi & Bhattacharjee, Suparna. (2023)Using the wet chemical precipitation approach, semiconductor nanoparticles with a core/shell configuration of cadmium selenide (CdSe) and zinc oxide (CdSe/ZnO) have been produced. The nanoparticles are capped with polyvinyl alcohol (PVA). From 9.5 to 11.5 was the pH range of the solutions. In order to determine the size of the CdSe nanoparticles, the Brus Equation was used. Core CdSe samples analyzed by UV-Visible spectroscopy exhibit blue-shifted absorption edges in the 342-377 nm range, in contrast to the 712 nm observed in bulk CdSe, and red-shifted absorption edges in the 346-357 nm range, in contrast to the core sample onto which the shell is deposited. Compared to bulk CdSe, which has a band gap value of 1.74 eV, the band gap values for CdSe core nanoparticles ranged from 3.70 to 3.90 eV. Nanoparticles with a core and a shell also have band gap values between 3.75 and 3.80 eV. The core samples show an excitonic emission peak at around 323 nm, whereas the core/shell samples show an emission peak at about 324 nm, according to the photoluminescence spectra. Based on XRD spectra, we know that the core CdSe sample had an average crystallite size of 11–31 nm, and that the core/shell CdSe/ZnO sample had an average crystallite size of 62–69 nm. The scanning electron microscopy results showed that both the core and core/shell samples were rather spherical. According to the results of the HRTEM investigation, the size of the core/shell nanoparticles ranged from 20 to 50 nm, while the size of some of the core nanoparticles was 3 to 8 nm.

Saidzhonov, B.M. et al., (2019) Ultrathin CdSe/CdS, CdSe/CdS/ZnS, and CdSe/ZnS core-shell nanoplatelets were studied for their morphology, structure, and optical characteristics in relation to the shell material's composition and thickness. It has been shown that, when ZnS and CdS shells are grown on ultrathin CdSe nanoplatelets with excitonic absorption at 463 nm, respectively, flat CdSe/CdS and CdSe/CdS/ZnS core-shell heterostructures are produced. By modifying the shell's composition and thickness, the initial excitonic transition may be tuned within a range of 510-635 nm. The CdSe/CdS and CdSe/CdS/ZnS core-shell nanoplatelets exhibited narrow emission bands with a width of around 18-21 nm, despite their high lateral diameters. It is shown that the emission width of CdSe/ZnS heterostructures is wider than that of CdSe/CdS and CdSe/CdS/ZnS heterostructures, and it is also thickness dependant. Potentially useful in light-emitting diode and laser applications is the ability to manipulate the electrical structure of 2D core-shell nanoparticles by adjusting their shell's thickness and composition.

©IJRASET: All Rights are Reserved | SJ Impact Factor 7.538 | ISRA Journal Impact Factor 7.894 |

Quang, Nguyen. (2010) we have synthesized CdSe and CdSe/ZnS core/shell quantum dots using a traditional, non-coordinated-based approach in this study. In the absence of trioctylphosphine oxide (TOPO), a CdSe/ZnS core/shell structure was effectively produced in a non-coordinating solvent for the first time. Using UV-Vis absorption spectroscopy, photoluminescent (PL) spectroscopy, and transmission electron microscopy (TEM), the resulting CdSe nanocrystals were studied. The results showed that a series of CdSe particles with diameters ranging from 1.9 to 3.5 nm were successfully produced, matching the first peak of the absorption spectra in the 450-570 nm range. Coating the previously synthesized CdSe core with different layers of ZnS allowed for the fabrication of the CdSe/ZnS core/shell structures. The photoluminescence of these CdSe/ZnS semiconductor quantum dots was much higher than that of the initial CdSe cores. Due to their small width, CdSe/ZnS quantum dots exhibit ideal dispersibility, high fluorescence, and a uniform size distribution when manufactured. These are necessary for a variety of possible uses, including photovoltaic applications, cellular imaging, and biological sensing.

Badr, Y. & Mahmoud, Mahmoud. (2006) The particle size of ZnSenanocrystallites was controlled by using a polyvinyl alcohol (PVA) matrix. The particle size decreased significantly when the ratio of zinc (Zn) to selenium (Se) ions increased. Photoluminescence, which underwent a blue shift with particle size reduction, and UV-vis absorption measurement were used to track the particle size decline. The use of X-ray diffraction (XRD) allowed for the characterization of particle size. The Raman spectra revealed that the peak location of the line centers (LO) mode is red-shifted from 239 to 234 cm(-1) and that the full-width at half-maximum (FWHM) also rises with increasing particle size. To investigate how the size of ZnSe NPs affected the PVA matrix, electrical measurements and Fourier transform infrared spectra (both overtone and normal) band vibration were used.

Chistyakov, A. et al., (2006) Using visible-laser stimulation over a broad spectrum of flux densities, the core-shell optical characteristics of CdSe/ZnS semiconductor nanocrystals are investigated. The films with a very high concentration of nanocrystals maintain the dimensional quantization effect, as shown. When the concentration of nanocrystals is high and the dipole moment is related to the asymmetry of the nanoparticles, the absorption and luminescence peaks in films with a low concentration of nanocrystals and solutions undergo a strong bathochromic shift with respect to the peak positions in the corresponding spectra. The film thickness determines the range of shifts, which may be anywhere from 35 to 50 nm. Even when the laser power is increased to 1×10^1 W/cm², the luminescence spectra of the films do not alter. The nanoparticle films are subjected to laser action at intensities (5 × 10−1 × 109 W/cm2) greater than the damage threshold.

Sharma, Himani et al., (2006) The shape of CdSe nanoparticles with organic molecules attached is the topic of this study. Using varying ratios of Cd:Se as starting materials, semiconducting CdSe nanoparticles ranging in size from 5 to 16 nanometers are created by combining a CdO precursor with a trioctyl phosphine (TOP) or trioctyl phosphine oxide (TOPO) cap. Highly luminous nanoparticles with a size of about 5 nm are produced at an ideal ratio of Cd/Se-2:1. Particle size, photoluminescence (PL) intensity, and optical absorption (UV-VIS) are all affected by the Cd/Se precursor ratio, which may be as varied as 0.5:1, 1:1, and 3:1. To find the system's crystallinity and stoichiometry, X-ray photoelectron spectroscopy (XPS) and X-ray diffraction (XRD) are used, respectively. The strong quantum confinement concept is shown to be in perfect agreement with the blue shifts of the optical absorption edge that occur simultaneously with the shrinkage of CdSe nanocrystals, as measured by XRD relative to the bulk semiconductor. Compared to the theoretical prediction derived from the strong quantum confinement paradigm, the optical edge shifts seen in CdSenanocrystallites by transmission electron microscopy (TEM) are noticeably larger. We can make sense of this by looking at the agglomeration effects that have been shown in TEM images of CdSenanocrystallites. Consequently, a number of TOP/TOPO passivated nanocrystals come together to create a nano-sized CdSe growth island.

III. RESEARCH METHODOLOGY

A. Data design

This study used a controlled experimental design to compare structural, optical and stability effects of different shelling strategies on CdSe nanocrystals. Four sample groups were prepared under identical base conditions with systematic variation only in shell composition and processing parameters.

B. Sample size

Sample sizes were chosen to provide sufficient statistical power for group comparisons while maintaining practical synthesis throughput. Total sample size 125 synthesized nanocrystal samples split by group.

C. Data analysis

The experimental data were analyzed using both descriptive and inferential statistics to evaluate the impact of shelling on CdSe nanocrystals.

TEM and XRD data were processed to determine particle size, crystallite size, and lattice strain, while optical spectra provided absorption, emission peaks, FWHM, and quantum yield values. TRPL decays were fitted with bi-exponential models to extract fast and slow lifetime components, and fitting accuracy was confirmed with χ^2 values.

Mean ± standard deviation was reported for all parameters, and group differences were tested using one-way ANOVA with Tukey's post-hoc tests or Kruskal–Wallis where assumptions were not met. Photostability trends were assessed through repeated-measures analysis, and correlations were examined between structural features (e.g., shell thickness, strain) and optical performance (e.g., QY, lifetimes). A significance level of $p < 0.05$ was applied, ensuring reliability and robust interpretation of the results.

IV. DATA ANALYSIS AND INTERPRETATION

Table 1: Sample set and synthesis parameters

Sample ID (group)	No. of replicates	Core/Shell structure	Typical precursor ratio (Cd:Se : shell precursors)	Shelling method	Reaction temp (°C)	Growth time (min)
C-01 … C-25 (Control)	25	CdSe (core only)	1 : 1	— (no shell)	220	30
Z-01 … Z-35 (ZnSe)	35	CdSe / ZnSe (single shell)	1 :1 : 2 (Cd:Se : Zn precursor)	Successive ionic layer adsorption (SILAR)	200	40
S-01 … S-35 (CdS)	35	CdSe / CdS (single shell)	1 :1 : 2 (Cd:Se : S precursor)	SILAR	210	45
D-01 … D-30 (Double)	30	CdSe / ZnSe / CdS (double shell)	1 :1 :2 : 2 (Cd:Se:Zn:S)	Sequential SILAR (ZnSe then CdS)	200 → 210	40 → 40

Table 1 outlines the distribution of the 125 synthesized samples across four groups: CdSe core-only (25), CdSe/ZnSe (35), CdSe/CdS (35), and CdSe/ZnSe/CdS double-shell nanocrystals (30). The synthesis parameters highlight that the control samples were grown at 220 °C without any shelling, while the ZnSe- and CdS-coated samples were fabricated using the successive ionic layer adsorption and reaction (SILAR) method. The reaction conditions differ slightly, with ZnSe shelling performed at 200 °C for 40 minutes, CdS at 210 °C for 45 minutes, and the double-shelling involving sequential deposition of ZnSe followed by CdS at progressively optimized temperatures. These parameters demonstrate a controlled and systematic approach to ensure reproducibility, with precursor ratios adjusted to favor successful shell growth. This setup provides a strong foundation for comparing the structural and photo physical modifications induced by different shelling strategies.

Table 2: Structural characterization (XRD, TEM) — average ± SD

Property	CdSe (control) (n=25)	CdSe/ZnSe (n=35)	CdSe/CdS (n=35)	CdSe/ZnSe/CdS (n=30)
Mean particle diameter (TEM, nm)	3.8 ± 0.4	4.6 ± 0.5	5.0 ± 0.6	5.8 ± 0.6
Size distribution (σ, nm)	0.6	0.7	0.8	0.7
XRD main peak (2θ, °) (wurtzite-type reference)	25.3 ± 0.2	25.1 ± 0.2 (slight shift)	24.9 ± 0.2 (shift)	24.7 ± 0.2
Crystallite domain (Scherrer, nm)	3.6 ± 0.5	4.3 ± 0.6	4.7 ± 0.7	5.4 ± 0.7
Lattice strain ($\times 10^{-3}$)	2.8	2.1	1.9	1.5
Shell thickness (nm, measured by TEM)	—	0.4 ± 0.1	0.6 ± 0.2	ZnSe:0.4, CdS:0.6 (total ~1.0)

Table 2 shows that the mean particle size increased progressively from 3.8 nm in CdSe core-only to 5.8 nm in the double-shelled CdSe/ZnSe/CdSNano crystals, confirming successful shell deposition. XRD peak shifts toward lower angles in the shelled samples reflect lattice expansion due to incorporation of ZnSe and CdS layers.

©IJRASET: All Rights are Reserved | SJ Impact Factor 7.538 | ISRA Journal Impact Factor 7.894 |

The crystallite size calculated using the Scherrer equation also increased, aligning with TEM observations. Moreover, lattice strain values decreased steadily from 2.8 $\times 10^{-3}$ for bare CdSe to 1.5 $\times 10^{-3}$ for the double-shelled samples, suggesting that shelling effectively relieves surface stress. TEM measurements also confirmed the shell thickness, with ZnSe contributing ~0.4 nm, CdS ~0.6 nm, and the double-shell combining both. These results indicate that shelling improves crystal quality, enhances stability, and provides more uniform growth.

Table 3: Steady-state optical properties in PVA films (room temperature)

Optical parameter	CdSe (control)	CdSe/ZnSe	CdSe/CdS	CdSe/ZnSe/CdS
Absorption peak (nm)	560	565	570	575
PL (photoluminescence) peak (nm)	575	580	585	590
PL full width at half maximum (FWHM, nm)	45	35	30	28
Stokes shift (nm)	15	15	15	15
Absolute quantum yield (QY, %) — measured in PVA film	25 ± 3	48 ± 4	55 ± 4	68 ± 5
PL intensity (relative, normalized to control = 1.0)	1.00	2.1	2.6	3.5

Table 3 compares the absorption and emission characteristics of the Nano crystals embedded in PVA. The absorption edge and PL peaks red-shift progressively with shelling, consistent with increased particle size. More importantly, the photoluminescence full width at half maximum (FWHM) narrowed significantly from 45 nm in bare CdSe to 28 nm in the double-shelled sample, indicating enhanced spectral purity. The quantum yield (QY) improved dramatically, rising from 25% for the core-only Nano crystals to 68% for the double-shell, confirming the role of surface passivation in suppressing non-radioactive recombination. Relative PL intensity followed the same trend, with the double-shell samples emitting 3.5 times more intensely than the control. These findings reveal that the shell structures not only improve efficiency but also lead to brighter and more stable emission in the polymer matrix.

Table 4: Time-resolved PL (TRPL) decay analysis (single- / bi-exponential fits)

Parameter	CdSe (control)	CdSe/ZnSe	CdSe/CdS	CdSe/ZnSe/CdS
Average lifetime $\langle\tau\rangle$ (ns)	12.0 ± 0.8	18.0 ± 1.1	22.0 ± 1.2	30.0 ± 1.5
Fit model	bi-exp	bi-exp	bi-exp	bi-exp
τ_1 (ns) (fast component)	3.5 (A_1=0.62)	4.2 (A_1=0.48)	5.0 (A_1=0.40)	6.0 (A_1=0.32)
τ_2 (ns) (slow component)	18.5 (A_2=0.38)	28.5 (A_2=0.52)	36.0 (A_2=0.60)	52.0 (A_2=0.68)
χ^2 (goodness of fit)	1.05	1.03	1.02	1.01

Table 4 presents the PL lifetime dynamics, which further reinforce the role of shelling in enhancing radioactive recombination. The average lifetime of CdSeNano crystals increased from 12 ns for the core-only to 30 ns for the double-shell structures. The biexponential fits reveal a decrease in the amplitude of the fast decay component (τ_1), associated with surface trap-mediated recombination, and an increase in the slow component (τ_2), corresponding to radioactive recombination from well-passivized excitons. Specifically, τ_2 extended from 18.5 ns in CdSe to 52 ns in double-shelled Nano crystals, with its relative contribution rising from 38% to 68%. The consistently low χ^2 values confirm good fitting accuracy. These results clearly show that shelling prolongs exciton lifetimes and suppresses non-radioactive channels, thereby enhancing luminescence efficiency.

Table 5:Photo stability, thermal behavior and film/matrix metrics (PVA matrix)

Metric	CdSe (control)	CdSe/ZnSe	CdSe/CdS	CdSe/ZnSe/CdS
Photostability: PL intensity retained after 1000 min (solar-sim., %)	40 ± 3	65 ± 4	72 ± 4	85 ± 3
Thermal decomposition onset (TGA onset, °C)	220 ± 3	240 ± 4	250 ± 4	270 ± 4
PVA film thickness (µm)	150 ± 10	150 ± 10	150 ± 10	150 ± 10
Film RMS roughness (AFM, nm)	12.0 ± 1.5	8.0 ± 1.0	6.0 ± 0.9	4.0 ± 0.7
Dispersion quality in PVA (qualitative)	Fair	Good	Good	Excellent
Water uptake effect on PL after 24 h immersion (% PL retained)	60 ± 4	75 ± 3	78 ± 3	88 ± 2

©IJRASET: All Rights are Reserved | SJ Impact Factor 7.538 | ISRA Journal Impact Factor 7.894 |

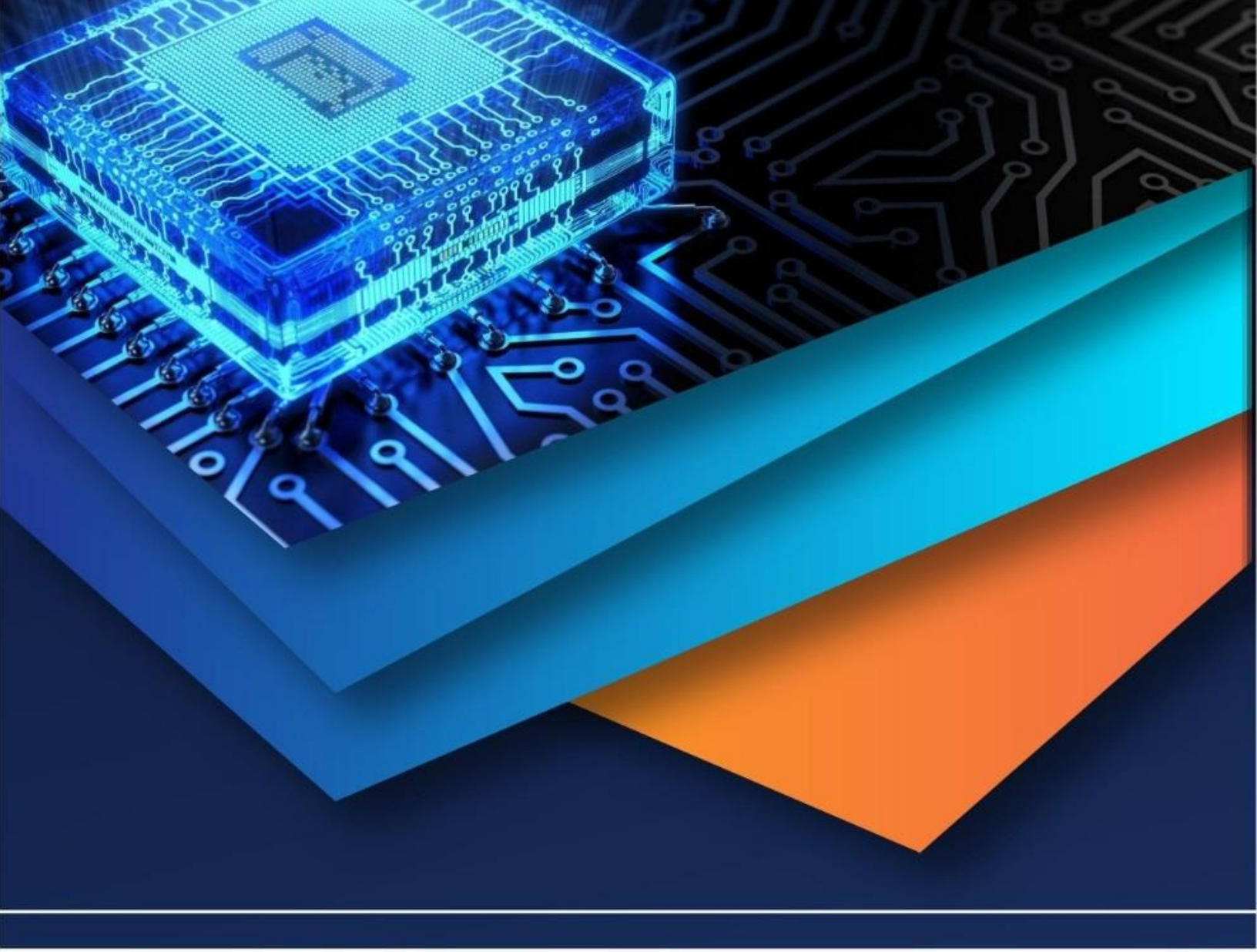
Table 5 emphasizes the improvements in environmental stability and film quality upon shelling. Bare CdSe nanocrystals retained only 40% of their PL intensity after 1000 minutes of solar-simulated irradiation, whereas the double-shelled samples retained 85%, demonstrating superior photostability. Thermal analysis revealed higher decomposition onset temperatures for shelled samples, with the double-shell stable up to 270 °C compared to 220 °C for the core-only. AFM studies showed smoother films for shelled nanocrystals, with RMS roughness decreasing from 12 nm to 4 nm, indicating improved dispersion in PVA. The qualitative evaluation confirmed that shelling enhanced matrix compatibility, with double-shelled samples showing excellent distribution. Additionally, the water-resistance of PL was higher in the double-shell (88% retention) compared to the core-only (60%), confirming their superior environmental robustness. Overall, these results highlight that ZnSe and CdS shelling not only improves optical performance but also enhances thermal, morphological, and environmental stability in polymer matrices.

V. CONCLUSION

The comparison of ZnSe and CdS shells on CdSe nanocrystals embedded in a PVA matrix highlights the delicate balance between structural compatibility and photo physical performance. ZnSe shells, owing to their wider bandgap and smaller lattice mismatch with CdSe, contribute to efficient passivation of surface states, leading to strong, sharp photoluminescence and high structural coherence. CdS shells, on the other hand, allow for thicker over layer formation, enhancing environmental and photo-stability, while simultaneously inducing strain and partial carrier delocalization that manifest as red-shifted and broadened emission features. The incorporation of these core/shell Nano crystals into a PVA matrix further stabilizes the nanostructures, prevents aggregation, and enables processable thin films for device applications. Taken together, the structural and photo physical outcomes suggest that ZnSe shells are advantageous for applications requiring narrow and intense emission, whereas CdS shells are better suited for scenarios demanding long-term stability and broader spectral response. The interplay between shell composition, lattice effects, and polymer encapsulation thus offers a versatile platform for tuning the optical properties of CdSeNano crystals, providing valuable insights for the design of next-generation optoelectronic and photonic devices.

REFERENCES

[1] J. Zhang, C. Li, J. Li, and X. Peng, “Synthesis of CdSe/ZnSe core/shell and CdSe/ZnSe/ZnS core/shell/shell nanocrystals: Surface-ligand strain and CdSe–ZnSe lattice strain,” Chem. Mater., vol. 35, no. 3, pp. 1–9, 2023.
[2] P. Boro and S. Bhattacharjee, “Effect of variation of pH and shell thickness upon the optical and structural characteristics of PVA capped CdSe and CdSe/ZnO nanoparticles,” J. Surf. Sci. Technol., vol. 1, no. 2, pp. 187–201, 2023.
[3] B. M. Saidzhonov, V. F. Kozlovsky, V. Zaytsev, and R. Vasiliev, “Ultrathin CdSe/CdS and CdSe/ZnS core-shell nanoplatelets: The impact of the shell material on the structure and optical properties,” J. Lumin., vol. 209, no. 3, pp. 1–9, 2019.
[4] M. Sebastian, B. Bhardwaj, A. Saran, P. Radhakrishnan, V. P. N. Nampoori, C. P. G. Vallabhan, and J. Bellare, “Effect of ZnS shell on optical properties of CdSe–ZnS core–shell quantum dots,” Opt. Mater., vol. 39, no. 1, pp. 1–9, 2015.
[5] M. Halajan, M. J. Torkamany, and D. Dorranian, “Effect of ZnSe concentration on the structural and optical properties of ZnSe/PVA nanocomposite thin film,” J. Phys. Chem. Solids, vol. 75, no. 11, pp. 1–7, 2014.
[6] S. Verma, S. Kaniyankandy, and H. Ghosh, “Charge separation by indirect bandgap transitions in CdS/ZnSe type-II core/shell quantum dots,” J. Phys. Chem. C, vol. 117, pp. 10901–10908, 2013
[7] M. Sharma and S. K. Tripathi, “Photoluminescence study of CdSe nanorods embedded in a PVA matrix,” J. Lumin., vol. 135, no. 3, pp. 327–334, 2013.
[8] N. Quang, “Synthesis and optical properties of CdSe nanocrystals and CdSe/ZnS core/shell nanostructures in non-coordinating solvents,” Adv. Nat. Sci.: Nanosci. Nanotechnol., vol. 1, no. 2, pp. 1–14, 2010.
[9] B. Goswami, S. Pal, and P. Sarkar, “A theoretical study on the electronic structure of ZnSe/ZnS and ZnS/ZnSe core/shell nanoparticles,” J. Phys. Chem. C, vol. 112, no. 2, pp. 1–12, 2008.
[10] M. Behboudnia and Y. Azizianekalandaragh, “Synthesis and characterization of CdSe semiconductor nanoparticles by ultrasonic irradiation,” Mater. Sci. Eng. B, vol. 138, no. 2, pp. 65–68, 2007.
[11] Y. Badr and M. Mahmoud, “Effect of PVA surrounding medium on ZnSe nanoparticles: Size, optical, and electrical properties,” Spectrochim. Acta A Mol. Biomol. Spectrosc., vol. 65, no. 1, pp. 584–590, 2006.
[12] A. Chistyakov, I. Martynov, K. Mochalov, V. Oleinikov, S. Sizova, E. Ustinovich, and K. Zakharchenko, “Interaction of CdSe/ZnS core-shell semiconductor nanocrystals in solid thin films,” Laser Phys., vol. 16, no. 2, pp. 1625–1632, 2006.
[13] H. Sharma, S. Sharma, G. Singh, and S. Shivaprasad, “Effect of ratios of Cd:Se in CdSe nanoparticles on optical edge shifts and photoluminescence properties,” Physica E Low-Dimens. Syst. Nanostruct., vol. 31, no. 1, pp. 180–186, 2006.
[14] D. Talapin, I. Mekis, S. Götzinger, A. Kornowski, O. Benson, and H. Weller, “CdSe/CdS/ZnS and CdSe/ZnSe/ZnS core-shell-shell nanocrystals,” J. Phys. Chem. B, vol. 108, no. 2, pp. 1–13, 2004.



10.22214/IJRASET

45.98

IMPACT FACTOR: 7.129

IMPACT FACTOR: 7.429

INTERNATIONAL JOURNAL FOR RESEARCH

IN APPLIED SCIENCE & ENGINEERING TECHNOLOGY

Call : 08813907089 (24*7 Support on Whatsapp)